Construction and Building Materials 407 (2023) 133452

Contents lists available at ScienceDirect

Construction and Building Materials

journal homepage: www.elsevier.com/locate/conbuildmat

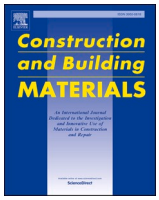

Performance evaluation of rail trackbed stiffness: pre and post stabilisation

Koohyar Faizi [a,*], Paul Beetham [a], Rolands Kromanis [b]

[a] Nottingham Trent University, Nottingham, United Kingdom
[b] University of Twente, the Netherlands

ARTICLE INFO

Keywords:
Railway
Trackbed stabilisation
Vision-based monitoring
Micro-piling
Track stiffness
Finite element

ABSTRACT

Excessive deflection of a rail in response to axle loading can lead to discomfort for passengers and increased wear of both railway structures and trains. These oscillations are often caused by poor trackbed stiffness which may be due to either soft subgrade and/or contaminated ballast. A variety of trackbed stabilisation (TBS) techniques are available to remediate soft subgrades and increase the safety of tracks within the railway network. Traditional TBS methods require track removal, which is expensive, disruptive and often inefficient maintenance works. Micro-piling, using screw piles installed between sleepers, is an innovative low disruption TBS technique. This paper investigates the performance of a soft subgrade and contaminated ballast section of rail line in the UK, before and after screw pile TBS. Pre and post remediation, a computer vision-based system was used to measure rail vertical deflections during train passages and then analysed to quantify the trackbed stiffness. Additionally, 3D finite element models are created and validated by the site measurements. The finite element models are used to simulate a range of different scenarios exploring how changes to the TBS piling layout and/or further works, such as ballast improvement could add further improvements or design efficiencies. Site measurements show TBS reduced rail deflection by 20–30%, indicating that micro-piling is an effective technique for soft subgrades. The finite element analysis revealed the efficiency of micro-piling is highly dependent on the conditions of ballast, strength of the ground at the pile toe, and the pile arrangement. When the aforementioned are optimised the rail deflection could be reduced to approximately 50% of the pre TBS condition.

1. Introduction

In ballasted railways passing train axles apply dynamic loads, as a repeated force from train axles which is supported by the combined stiffness of the track system. The track system comprises; the track structure of rail, fastenings and sleepers, and the trackbed comprising ballast (including sub-ballast if present) and subgrade. Low track bed stiffness results in high rail deflections, settlement of rails from design level, rapid deterioration in track quality and subsequent reduced reliability with increased maintenance costs over the asset lifespan [18]. Low strength natural ground is a fundamental cause of low track bed stiffness in ballasted railways and resulting excess rail deflections may either be from: (i) Quasistatic loadings where the train axle loads apply vertically downward and inadequate elastic stiffness may cause excessive strain in the subgrade; (ii) The transmission of Raleigh waves from high-speed trains which propagate slowly through soft ground which may lead to resonance and train instability. The train speed at which resonance occurs is called the critical speed [33,11].

When excess deflections are detected e.g., by specialist measurement trains, to prevent accidents, Temporary Speed Restrictions (TSRs) are implemented by operators. TSR of 75% of the critical speed is recommended until the trackbed is renewed [29]. Regular ballast tamping is one way to correct rail alignment and lessen rail deflections. Alongside negatives of cost and track possession time, tamping may disrupt the load-bearing structure and damage individual ballast grains [2]. Long-lasting forms of Track Bed Stabilisation (TBS) methods are preferred to ameliorate issues from soft subgrades such as: mass stabilisation with dry deep soil mixing; stabilisation with asphalt, geogrids; subgrade replacement [27,12,23]. Musgrave et al. [21] noted the advantages of using micro-piling, particularly in the form of screw piles, as a rapid installation and low disruption technique to execute TBS across a sequence of 6 to 8 h possessions. They also emphasise that the installation of screw (or helical) piles, in comparison to grouted/driven piles, produces less track movement and reduces contamination to ballast. Techniques to reduce the susceptibility of ballast to stiffness degradation or spreading from repeated cyclical loading may also be employed. This

* Corresponding author.
E-mail address: koohyar.faizi@ntu.ac.uk (K. Faizi).

https://doi.org/10.1016/j.conbuildmat.2023.133452
Received 1 June 2023; Received in revised form 15 August 2023; Accepted 19 September 2023
Available online 28 September 2023

may be through treatment of ballast with; binding materials such as resin or bitumen [4]; tensile reinforcement from geogrids [17]or lateral confinement with geocells (Wehbi et al., 2018). These may be included as part of a hybrid stabilisation approach where poor subgrade is first treated with micro-piling initially executed with minimum disruption across overnight possessions. Then if subsequent monitoring shows further improvements are required, a second phase of more disruptive work to improve the ballast using one of the above noted methods may follow on. An improved ballast condition enhances the effectiveness of micro-pile TBS to deliver further overall trackbed stiffness [7].

Track modulus is a basic parameter to measure the quality of a track. It is defined as the supporting force per unit length of the rail per unit deflection [30], and it is a function of both the load applied to the rail and the associated track displacement. The track modulus can be estimated from track deflection using the beam on an elastic foundation (BOEF) model [25]. Therefore, where the track deflection at locations affected by soft subgrade can be directly measured there is a means to quantify the track quality before and after TBS to quantify the degree of improvement. Furthermore, where the ground profile and ballast properties are adequately characterised, there is similar potential for geotechnical analysis e.g., Finite Element (FE) analysis to predict rail level movements before and after TBS.

Several measurement techniques exist for measuring track deflections. Non-contact measurement technologies allow accurate measurement without physically attaching sensors to the host structure [22]. The contact measurement systems generally encompass high precision displacement transducers such as linear variable differentiation transformers and string potentiometers. The main disadvantage of these systems is their dependence on a reference because they measure displacement between a point on the structure and a point where they are fixed. Vision Based Monitoring (VBM), as a form of non-contact measurement system, presents a promising tool for measuring displacements in civil structures [6,15]. In comparison to contact displacement sensors, VBM systems have low instrumentation costs, are easy to install and offer a wide range of measurement capacity (e.g., measurement collection frequency and spatial resolution) [38]. A VBM system to measure railway track displacements was first explored by Bowness et al. [5] and Priest et al. [26] as a means of gathering dynamic railway deflections from passages of trains. Since then, VBM systems have been used in combination with geophones and (or) accelerometers to study ground deformations [26]and transition zones [36], as well as longitudinal rail displacements [20].

This paper investigates the improvement of poor track quality using micro-pile TBS at a soft subgrade with contaminated/dirty ballast, site in Berkshire, UK. Vertical deflections of the rail were recorded with a VBM system before and after TBS implementation. Using the VBM measurements for calibration, a three-dimensional (3D) FE model was created to assess the effectiveness of the micro-pile TBS technique in reducing track level deflections from the initial condition. The FE analysis was then extended to consider how subsequent improvements to the dirty ballast properties and / or longer piles embedded into stiffer strata would further improve track bed stiffness and also established an optimal layout of micro-piles with fewer piles. This method establishes a framework for optimal TBS design and validation, aimed at increasing confidence in micro-pile use with future efficiencies.

2. Micro-pile TBS and study site

2.1. Micro-pile

Micro-piles, constructed using steel shafts with helical flights (the diameter is circa 300 mm), are installed between sleepers either within the four foot or sleeper ends (Fig. 1). It is suggested that micro-piling reduces rail deflections by transferring stresses from rail traffic onto the pile head, with arching generated within the ballast to span between pile centres, causing pile end bearing and shaft frictional resistance [21].

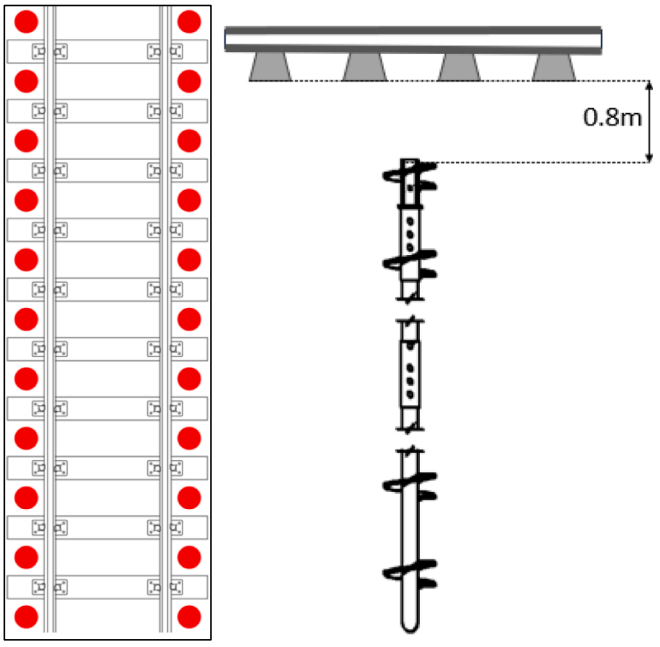

Fig 1. a) Plan view of proposed micro-piles spacing (arrangement of piles in red circles); b) Schematic of general assembly of micro-pile (Van Elle Ltd.). (For interpretation of the references to colour in this figure legend, the reader is referred to the web version of this article.)

The configuration of the micro-piles is dependant on project type, however; piling in alternate sleeper bays is suggested where minimum thickness of the granular layer (GH) below the sleeper bottom is greater than 0.5 m. Whereas, piling every alternate sleeper bay is not permitted if 0.4 m $\leq$ GH $<$ 0.5 m and piles should be installed every sleeper bay Musgrave et al. [21].

It worth nothing that the above minimums were not presented as outputs from any specific trial/s or geotechnical analysis and may be based on engineering instinct as opposed to direct evidence.

The micro-piles in this study were specifically developed by the piling contractor (Van Elle Ltd.) for TBS. Installed in pairs at every interim sleeper (see Fig. 1a) using road/rail-mounted plant (see Fig. 2), the system utilises a modified micro-pile with a patented pile cap designed to aid load transfer. The pile cap section includes two flights to increase the pile cap area to further enhance shear resistance to vertical loads and provide lateral stability of the pile head. The steel pile cap is typically installed at a depth of 0.8 m below the existing sleeper bottom layer in order to avoid the disruption of the regular ballast tamping maintenance [7]. The pile toe section consists of two flights, designed to ensure secure embedment into the firmer soils at depth (see Fig. 1b). For the current site, a 10 m long pile was determined in the scheme design. The authors were not the scheme designers, but it is understood the length was selected intending to pass through the weakest soils, embedding the lower two flights within firmer layers underneath. Further details of the ground conditions are presented in the following sections.

2.2. Study site

The site is an at-grade double-track railway section in Berkshire, England and comprises a straight section near to a level crossing and station. Investigations by the asset owner revealed excessive vertical track deflections on the up line which meant a TSR had been put in place.

The trackbed system comprises flatbottom rail and concrete sleepers

Fig 2. Trackbed stabilisation with micro-piling (Van Elle Ltd.).

constructed on a 1 m depth of clay/coal dust contaminated ballast (dirty ballast). The underlying ground conditions had been established by a series of window sample and dynamic probes advanced to 10 m below ballast level, identifying alluvial deposits of silty clay interbedded with amorphous peat. The window samples identified the cohesive ground was soft to very soft and the dynamic probes N100 values ranged between 1 and 3 indicating an undrained shear strength ranging between 7 and 35kN/m^2 across the site and generally increasing with depth.

With the soft subgrade condition identified, it was intended to first employ TBS using micro-piles, on overnight possessions and without the need for track removal. Thereafter, there was provision for the contaminated ballast to be renewed and improved with geocells if needed at a later extended possession. The 10 m long micro-piles were installed in pairs (Fig. 1), utilising a road/rail-mounted plant for installation (as shown in Fig. 2).

2.3. Vision-based displacement monitoring systems

The vision-based monitoring system is, generally, composed of an image acquisition device(s) (e.g., camera(s)), computer, and an image processing software (i.e., computer vision algorithms). Applying a vision-based system for track deflection monitoring requires setting up a camera in a stable location, focusing it on visual targets, which are attached to the track components (i.e., rail and sleeper), and deriving the structural displacement through target tracking [8].

In this study, a computer vision algorithm was used to analyse images (video frames) including the predefined regions of interest captured by the digital camera. The target based VBM system comprising a modified GoPro camera, equipped with a zoom lens, was used for measuring the vertical deflections of the track subjected to train passages (i.e., passenger and freight trains) at site. The camera was set up 5 m from the track and recording at 120 Hz. VBM set-up with targets attached to the rail components are illustrated in Fig. 3. The camera, mounted on a tripod, was stabilised to reduce vibration caused by traffic or wind during the testing process. Track vertical displacements before and after TBS were compared to assess the track performance after its strengthening with micro-piling. The VBM results are used to calibrate Finite Element (FE) models and optimise TBS design.

For this study displacements of the rail and sleepers were measured. Results provide information about voids in the track, rail deflections for track modulus calculation and for comparison of deflection before and after TBS [8].

2.4. The track modulus

The BOEF is a prevalent and simple numerical mode for displacement of a railway track [19] with the most common methods using the Winkler approach [24]. The differential equation for a BOEF analysis is derived with the vertical deflection of the rail w at distance x along a beam with bending stiffness EI on an elastic foundation and a system support modulus (stiffness per unit length) :

$$EI + \frac{d^4 w(x)}{dx^4} + kw(x) = 0 \tag{1}$$

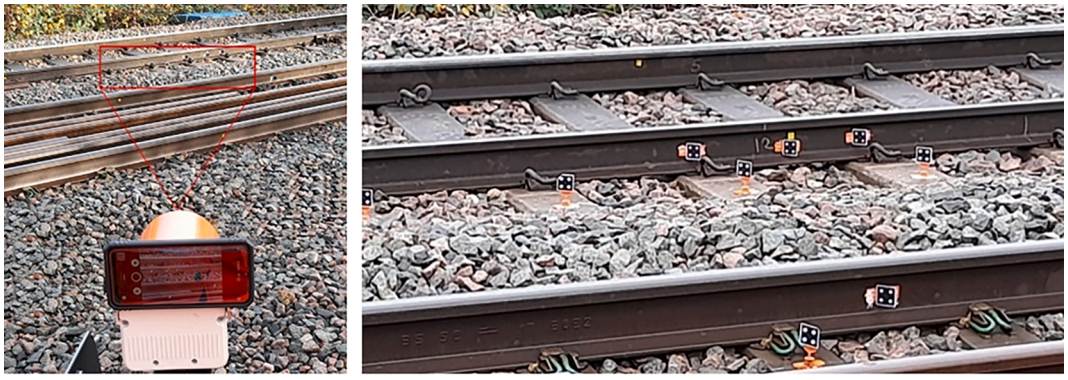

(a) (b)

Fig 3. VBM at site (a) camera setup, and (b) visual targets.

The vertical deflection of the rail to a single point load P is calculated as follows:

$$\delta(x) = \frac{P}{2k_{sys}L} e^{-(x/L)} \left(\cos\frac{x}{L} + \sin\frac{x}{L}\right) \quad (2)$$

where L is the characteristic length of rail.

$$L = \sqrt[4]{\frac{4EI}{k_{sys}}} \quad (3)$$

Where support system modulus (k_{sys}) is combination of the rail pad modulus ($k_{railpad}$) and the trackbed modulus ($k_{trackbed}$), and given by formula for springs in series:

$$\frac{1}{k_{sys}} = \frac{1}{k_{railpad}} + \frac{1}{k_{trackbed}} \quad (4)$$

In the equations above, equivalent dynamic load (P) was considered to be the magnitude of moving loads greater than the wheel loads at rest. The dynamic equivalent load was calculated by applying a dynamic wheel load factor derived using the averages method presented by Van Dyk et al. [35].

In this paper, the support system modulus was calculated from the sleeper spacing (s), although the measurements were applied to the sleeper only instead of along the rail. The track modulus was also calculated with the rail type UIC 60 and based on the displacement caused by double wheel loads, as a single load may not be representative of the track response [37].

3. Numerical modelling

The dynamic response of a trackbed under train loading before and after piling, then design optimisation (subgrade/ballast conditions and pile arrangement) was investigated using commercially available 3D FE analysis software .

3.1. Geometry and material properties

Fig. 4 presents the general arrangement of the 3D FE model, with a 2D cross-section. The length of the ballasted track is 80 m including 133 concrete sleepers spaced at 0.6 m centre to centre, with rectangular sleepers of cross-section 0.3 × 0.3 m and length of 2.5 m. To simplify the model and save computation time, only a single track, rather than both up and down lines were included in the FE models; this also reflected the

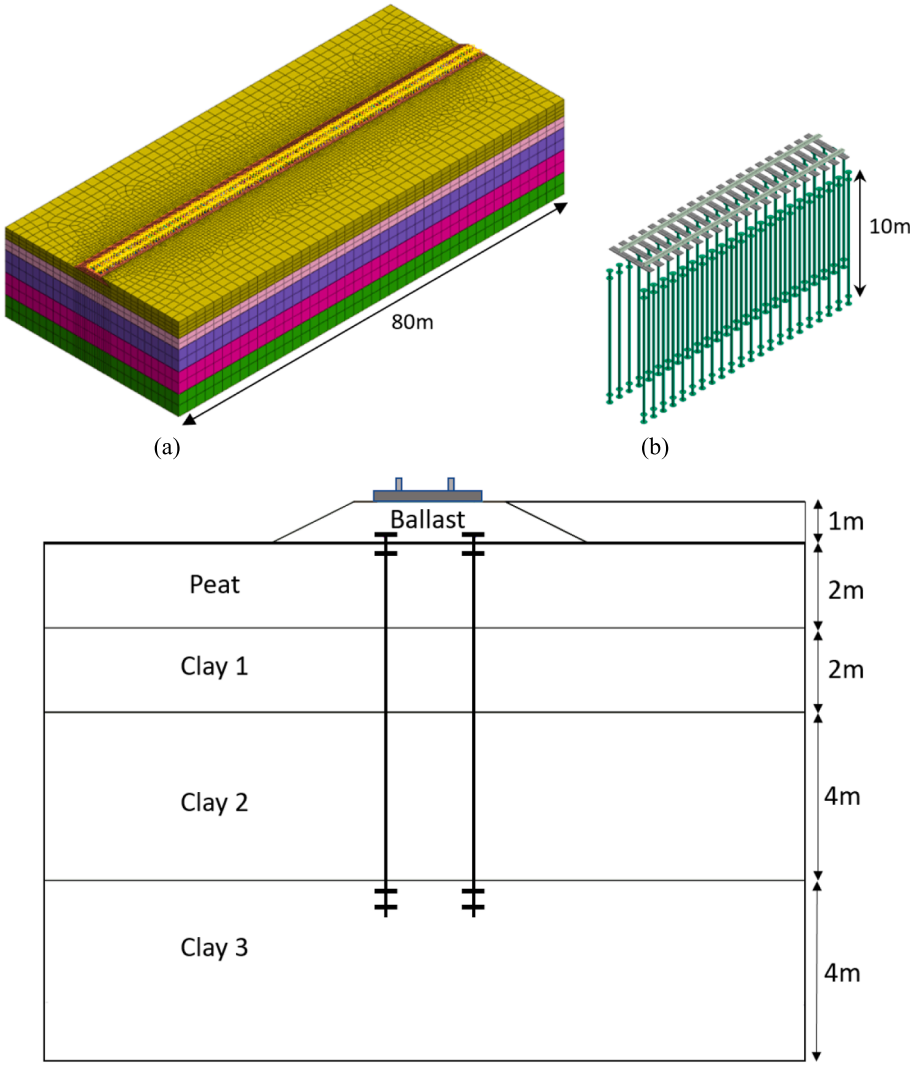

Fig 4. The railway track: a) track FE 3D model; b) and embedded micro-piling arrangement; c) Cross-section of ballasted track section.

fact that no VBM data was collected as trains passed in opposing directions.

Three different scenarios were modelled with Scenario 1 comprising the base numerical model established from knowledge of the track system, operator provided data i.e., automatic ballast sampling (ABS) and ground investigation reports and literature. The ground profile consists of a 1 m deep ballast layer (with side slope of 2H:1V), overlying a peat layer of 2 m, then 3 layers of clay (Clay1 = 2 m, Clay 2 = 4 m and Clay 3 = 4 m). As the ABS and ground investigation data was limited to particle size distributions, engineering descriptions and large failure strain probing, it was not considered suitable to directly determine the dynamic engineering properties needed. Instead, literature values from similarly described materials (dirty ballast/soft clay and peat; [29],Stark et al. [31]were used for scenario 1 values and then parametric analysis of the ballast and subgrade parameters were undertaken in Scenarios 2 and 3 respectively (Table 1).

3.2. Train loading configuration

A moving load finite element method-based approach, which is a sequence of discrete pulse loads at the rail nodes, was used to simulate a traveling train in accordance with the approach described by Araújo [3]. The moving loads were defined as triangular pulses of increasing force distributed across three consecutive loading nodes along the travel direction. In such a simulation, the spacing of the loading nodes (FE rail nodes) are divided by the train speed results to time step of calculation, and the software automatically applies it to the analysis model as a dynamic nodal [29]. Class 802 of Great Western Union (GWR) and class 166 Network Express Turbo passenger train services with average weight of each car 40–50 tons were operating in the route.

To save computing time and after initial analyses identified repeating the same load arrangement simply duplicates the same displacement trend, only the axle loads of three cars from the entire train were considered in the FE models. Fig. 5 illustrates the loading configurations including 6 bogies of three passenger cars for axial load of 120 kN and train speed of circa 100 mph.

To produce the natural transient phenomenon of wave propagation through the ground, time domain models were performed in the models [14,29]. The material damping of the FE model is characterised by the mass and stiffness proportional coefficients, using the Rayleigh damping which is dependant on the natural frequency [10]. The natural frequency of the FE model was obtained from the eigenvalues considering the subgrade reaction at the boundary of the layered material mesh. During the moving load simulation, the smaller time step is always selected based on the well-known Courant number (C_n) [9]to ensure the number remained below one, which is mathematically represented as follows:

$$C_n = \frac{\Delta t \times C}{L_{min}} \leq 1 \tag{5}$$

where, Δt is the time step, C is the train speed and L_{min} is the distance between two adjacent loading nodes.

The finite element size, model boundaries and time step were carefully selected to ensure the accuracy of results while balancing computational time efficiency. The nodes at the bottom boundary were fixed in all directions to simulate bedrock. The element size was estimated based on the smallest wavelength that allows the high-frequency motion to be simulated correctly. This meant that element sizes ranged from of 0.15 m to 1.8 m, with finer mesh used nearer to track level becoming coarser further away. Overall, the FE mesh consists of 102,611 elements. The viscous dampers are connected to the vertical boundaries of the model to absorb the incident S- and P-waves to represent infinite boundary conditions, as suggested by many researchers (e.g., Kouroussis et al. [14], Lysmer and Kuhlemeyer [16].

3.3. Track components

To model the continuous rail lines, one-dimensional I-beam sections extending across the length of the modelled track were used. Parameters relevant to UIC-60 rail section were used, and modelled as fixed to the sleepers by rail pads characterised by an elastic link (spring-like) element of stiffness equal to 100 MN/m [29]. All other track components (i.e., sleeper, ballast, interface and subgrade) were modelled using 3D solid elements.

The rail and sleepers were considered as linear elastic materials. The ballast and subgrade layer are assumed to be elastic in the current model due to the very short-term nature of the loading and low level of applied stress within the subgrade (parameters in Table 1).

In order to reduce the complexity of models and computation time, the micro-piles were represented by embedded beam elements with soil–pile interaction along the pile shaft and at the pile tip. The soil-pile interface was defined in SoftwareMidas-GTS [1] using Wizard interaction formula with three parameters of ultimate shear force, shear stiffness modulus, and normal stiffness modulus. In the absence of pile test data, the ultimate bearing resistance was adopted from the formula proposed by Tappenden et al. [34].

3.4. Field test measurement and analysis

For several days both before and after micro-piling work, repeated measurements of the track structure deflection were recorded by VBM during passage of rail traffic travelling at a range of speeds. This allowed a dataset of different train types / speeds to be compiled, permitting understanding of the range of and typical deflections trends for different rail traffic combinations; before after TBS. Non-stopping passenger and freight trains were operating approximately 90–100 mph (fast train) and 45–60 mph, respectively. Some of the measurements were for trains which were slowing on approach to the nearby train station (slow train), so speeds were not constant across data capture.

Example deflection trends for VBM of the rail web prior to TBS for both passenger (slow and fast) and freight trains are shown in Figs. 6 to 8. Freight trains associated with vertical maximum displacement up to 6 mm, whereas passenger trains ranged between 2.5 and 3.5 mm. As the track operator requires vertical deflection of < 2 mm to permit full speed passenger traffic at 125mph this aligned well with expectations and the need for the planned TBS work.

To aid comparison, Figs. 7 and 8 show example post TBS VBM trends

Table 1
Material properties of the TBS project.

Materials	Thickness (m)	Dynamic Young's modulus, E, (MPa)			Poisson's ratio, ν	Unit weight (kN/m^3)	Damping ratio, ξ
		Scenario 1	Scenario 2	Scenario 3			
Rail	–	210,000	210,000	210,000	0.3	76.5	–
Sleeper	–	30,000	30,000	30,000	0.2	20.15	0.02
Ballast	1	125	250	250	0.3	18.64	0.03
Peat	2	5.6	5.6	5.6	0.49	17.0	0.06
Clay 1	2	22.5	22.5	22.5	0.49	17.7	0.09
Clay 2	4	22.5	22.5	22.5	0.49	17.7	0.09
Clay 3	4	26	26	60	0.49	17.9	0.09

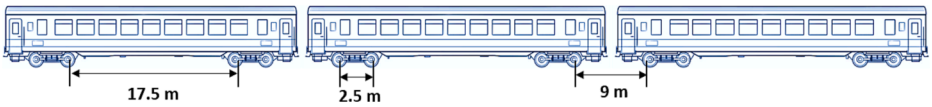

Fig 5. Loading configuration (not scaled).

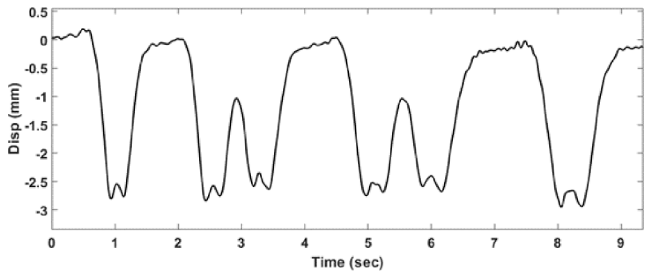

Fig 6. Vertical deflection of rail obtained by VB system, under passage of a passenger train with reducing speed stopping at station (average 22mph).

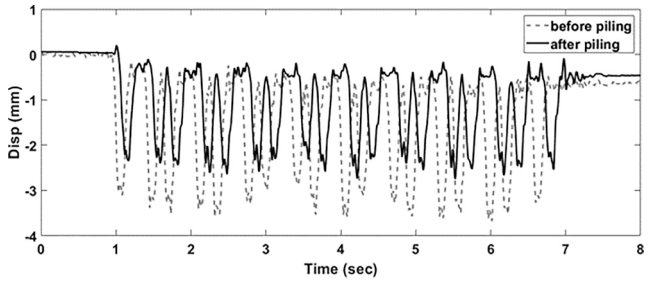

Fig 7. Vertical deflection of rail obtained by VB system, under passage of 3-coaches passenger trains with non-stopping at station, before piling and after piling.

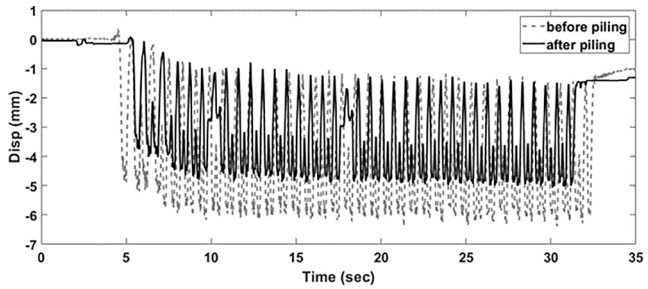

Fig 8. Vertical deflection of rail obtained by VB system, under passage of freight trains before piling and after piling.

recorded at the rail web for both passenger (slow and fast) and freight trains, alongside values recorded prior to TBS. Consideration of the full dataset showed consistent trends that when comparing similar train type and speed, there was a reduction in deflection in the pre and post TBS trends of 20–30% and some specific examples are discussed further.

Fig. 7 shows trends for fast passenger trains with 9 cars where pre-TBS the maximum range of downward deflection was approximately 3.5 mm and post TBS this had reduced by approximately 1 mm. Fig. 8 shows freight trains (46 and 35 wagons respectively) where the pre-TBS maximum displacement of 6 mm reduces to 4.8 mm. With a longer train it is interesting to observe that the level the rail rebounds to between axles moves progressively away from the zero datum with repeated cycles. After 31–32 s the datum for both pre and post TBS trends has offset vertically by approximately 1.3 mm and a similar observation was seen in Murray et al., [20]. The displacement offset may be from elastic deformation in the trackbed which takes some several minutes to fully recover, which was the conclusion of Murray et al. [20], however, the data collection was not long enough to confirm that in this study.

A common defect in ballasted tracks experiencing regions with excess deflection is “unsupported sleepers”, where differential settlement of the ballast can cause a void beneath some sleepers, so they are essentially suspended by the rail and clips (Sresakoolchai, J. and Kaewunruen, S., 2022). The potential for unsupported sleepers was investigated by comparing the vertical deflection of three neighbouring sleepers before and after TBS. These comparisons, (e.g., Fig. 9) showed the vertical deflection values obtained from neighbouring sleepers were relatively consistent, whereas presence of a void under one would show a step change. This suggests “unsupported sleepers” was not a significant issue at this site.

3.5. VBM data analysis

Fig. 10 shows the trackbed modulus calculated from VBM data as obtained for similar fast trains comparing 3 passages before with 3 passages after TBS. The values were calculated using the BOEF model to initially plot theoretical displacement versus length. Then determining the point where maximum theoretical deformation matches the ultimate deformation obtained by VBM, thus allowing the equivalent track modulus to be determined.

To ensure satisfactory track performance, a minimum track modulus of between 28 MPa [30] and 35 MPa [28] is needed and while post TBS values of 37–43 MPa do exceed that range, there is limited margin for long term deterioration.

3.6. TBS degree of improvement discussion

The VBM verified a reduction in deflection of 20–30% after TBS which demonstrated the soft subgrade condition has been improved and the post TBS trackbed modulus is satisfactory in relation to literature. However, expectations from other sites (e.g., [21] were that deflection from fast passenger trains post TBS would have been less and closer to a maximum of 1 mm and this is discussed further.

One reason that deflections are higher than expected could be the known presence of dirty ballast, contaminated with clay and coal which would soften the ballast and cause more deflection within this layer. Furthermore, contamination in the ballast may reduce the frictional strength of the ballast, lessoning the effectiveness of arching between piles resulting in more stress transfer to the soft peat subgrade.

A second possible reason for higher than anticipated deflection post piling, could be the stiffness of the layer which the pile tip embeds into. While the ground conditions were noted to become stiffer with depth, the maximum undrained shear strength of 35 kPa expected from the dynamic probes is still relatively low stiffness and may not provide the same resistance as that seen in the Musgrave et al. [21] study.

The following numerical modelling will consider how both the ballast and pile tip bearing strata stiffnesses would influence track level deflections.

3.7. FE analysis

The ground investigation data was useful in determining the ground profile and soil engineering descriptions, yet was limited in quality to derive strength / stiffness parameters at the small strains relevant to the applied dynamic loading. Therefore, the literature derived values

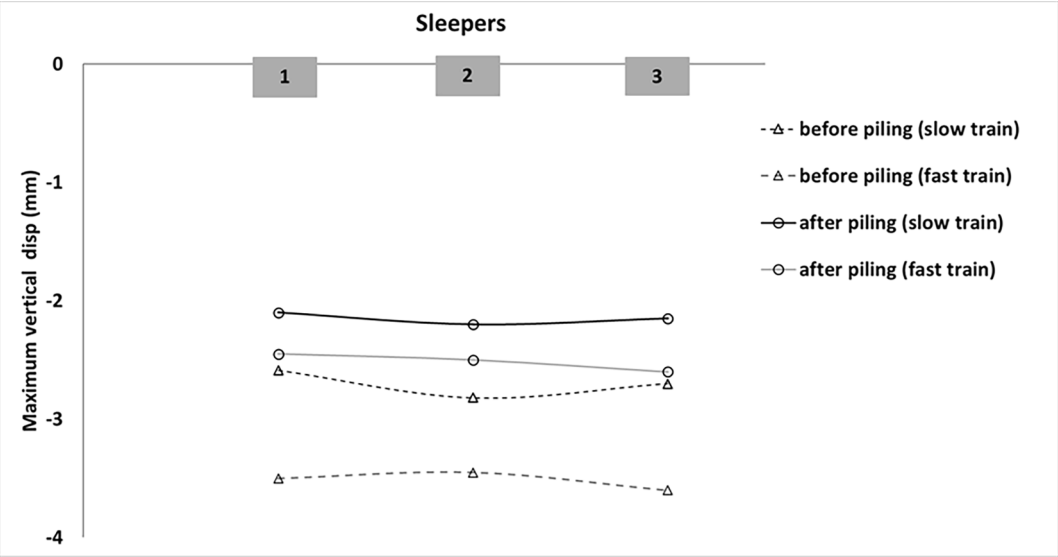

Fig 9. Vertical deflection of the rail at three neighbouring sleepers.

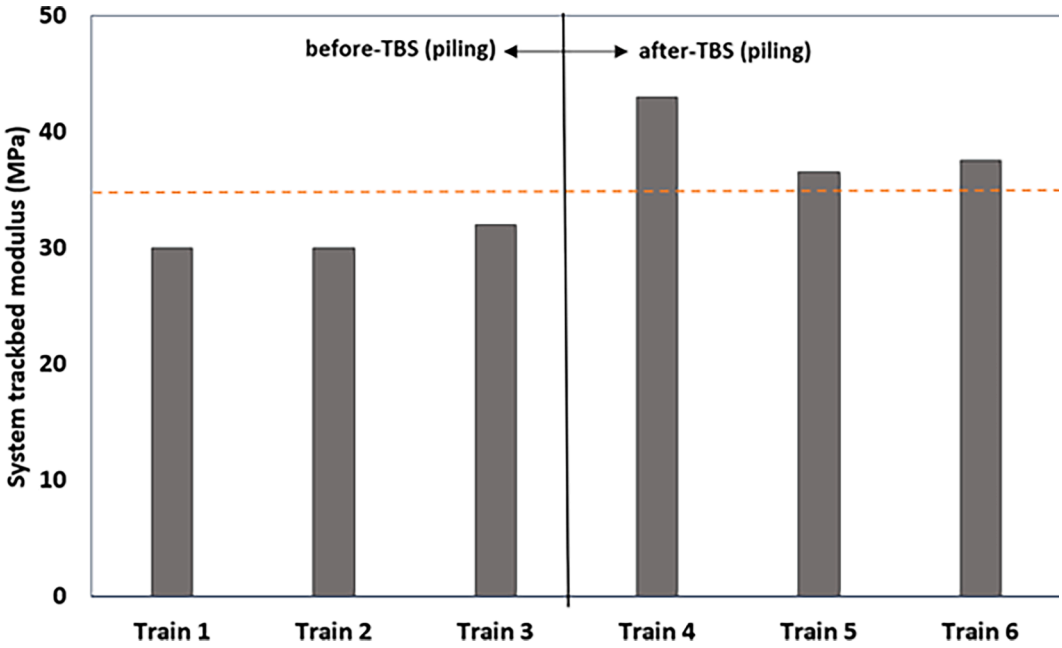

Fig 10. Comparison of trackbed modulus pre- and post-TBS.

(Table 1) would need careful validation from the VBM measurement, before confident use of the validated model in prediction of performance for other scenarios.

3.8. Validation using VBM measurements

Validation of the FE analysis was done by comparing the numerical model outputs of deflection with those collected from the VBM. Furthermore, the FE analysis was reviewed to ensure the assumed behaviour that the TBS system would transfer stress applied at trackbed level down to the pile toe were correctly modelled. The validated model was also used to estimate the critical speed of trains.

To output the FE model data in a format for comparison with the VBM data, the time-history response of rail deflection during train passage was calculated at the centre of track to eliminate boundary effects in the time domain models. As only the passage of three cars were simulated in the FE analysis, three cars of VBM plots were overlain against modelled data. FE results are compared with measured values obtained from VBM system before and after TBS, which show good agreement between measured and FE-predicted results (Fig. 11a and Fig. 11b.).

Figs. 12 and 13 comprise a long section view from the 3D FE model taken along the rail length. Fig. 12a and b shows the increase in stress as caused by the passing train axle (compression stress labelled as S-ZZ) where before TBS, a significant area within the peat layer shows stress increases of approximately 10 kN/m^2. After TBS this same region has reduced stress increase averaging approximately 5–6 kN/m^2 and instead a relatively widespread area radiating from around the pile toe shows increased stress by approximately 2 kN/m^2. This visualises the stress transfer caused by the installed piles and Fig. 13 a and b (which show the same view except as displacement contours) show the effect of this is to reduce displacement of the peat/overlying ballast from 3 to 3.5 mm to

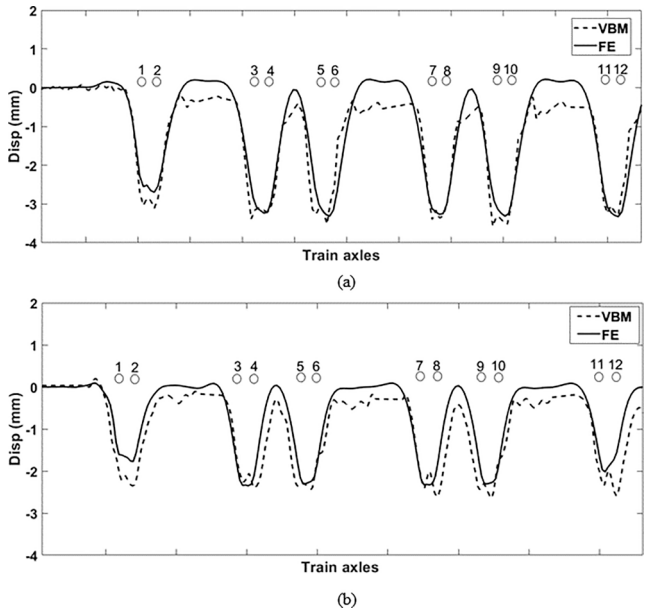

Fig 11. Comparison between FE predicted versus field measured deflection responses (VBM) at the track centre for: (a) train speed of about 100 mph before stabilisation; (b) train speed of about 110 mph after stabilisation. Numbered circles are representatives of train axles.

2–2.5 mm. Fig. 13.b also shows a widespread zone of small displacement of 0.5–1 mm extends around the piles and just past the toe indicating that smaller strains are mobilised in the stiffer soils at depth. Thus, the model shows the expected behaviour and is further validation it performs correctly.

3.9. Stiffness parametric study and optimum micro-pile layout

With the baseline FE model validated, the focus moved to investigating how the stiffness of the ballast and strata which the pile toe embeds within may change the rail level deflections. Thereafter, different pile layouts were explored to make a basic cost benefit analysis of increasing piles versus degree of improvement, with intent to identify an optimum. The study involved evaluating what the "critical speed" would be for each scenario investigated.

The initial model (Scenario 1) had included stiffness parameters for the ballast which accounted for its known contaminated / dirty ballast condition. Scenario 2 would model improvement of the ballast and is the same as scenario 1 except the ballast Young's modulus is increased to 250 MPa. Scenario 3 is as per scenario 2, except models the pile toeing into a stiffer subgrade layer so the Young's modulus of clay 3 was increased to 60 MPa.

These different scenarios allowed for a comprehensive exploration of the impact of ballast and subgrade conditions on trackbed deflection, providing valuable insights into the effectiveness of micro-piling in different scenarios.

3.9.1. Critical speed

As noted previously, when the train speed reaches the critical speed of the train–track–ground system, extraordinary large vibrations occur, leading to possible catastrophic track damages and train derailment. The trackbed stiffness has a fundamental influence on the critical speed with a softer condition associated with low critical speed. Therefore, the critical speed of the trackbed system before piling and then for scenarios 1–3 after piling was estimated using the validated FE model. Fig. 14 shows the maximum track downward deflection versus train speed for the aforenoted scenarios and in all cases, deflection increases with speed, until a peak deflection is seen at the critical speed i.e., about 60 m/s, 65 m/s, 70 m/s, and 80 m/s across the scenarios, before deflection reduces with further increase of train speed.

The results in Fig. 14 indicate that the critical speed progressively increases from 60 m/s for Scenario 1 (without micro-piling) up to the maximum 80 m/s for Scenario 3 with the inclusion of micro-piles, a clean ballast condition and competent layer at pile tip in subgrade layer.

The time-history displacement of the modelled train (Scenario 1 without micro-piling) based on various speed are shown in Fig. 15a. It can be seen that for low speed of 10 and 40 m/s, only quasi-static deflection (i.e., downward movement) appears when the load moves over the point of concern. In contrast, an oscillatory response occurs at higher speed of 60 and 80 m/s.

For the purpose of illustrating the impact of train speed on the track, the contour plots of total deflection along the track are shown in Fig. 15b (A-D) at four different speeds. It is noteworthy that the series of wave fronts radiating from the loading positions appear as a shockwave in the ground that is known as the Mach cone. Similar behaviour was also

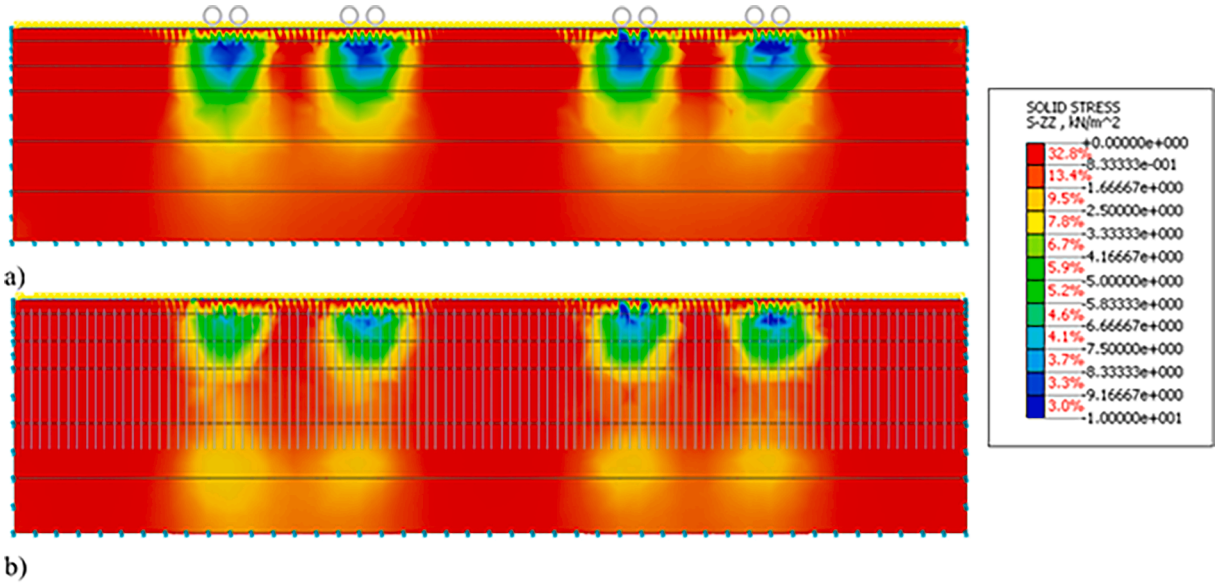

Fig 12. The contours of stress distribution in the longitudinal section under train axles (grey circles), obtained by FE, for models of; a) pre-micro-piling and b) post-micro-piling scenarios.

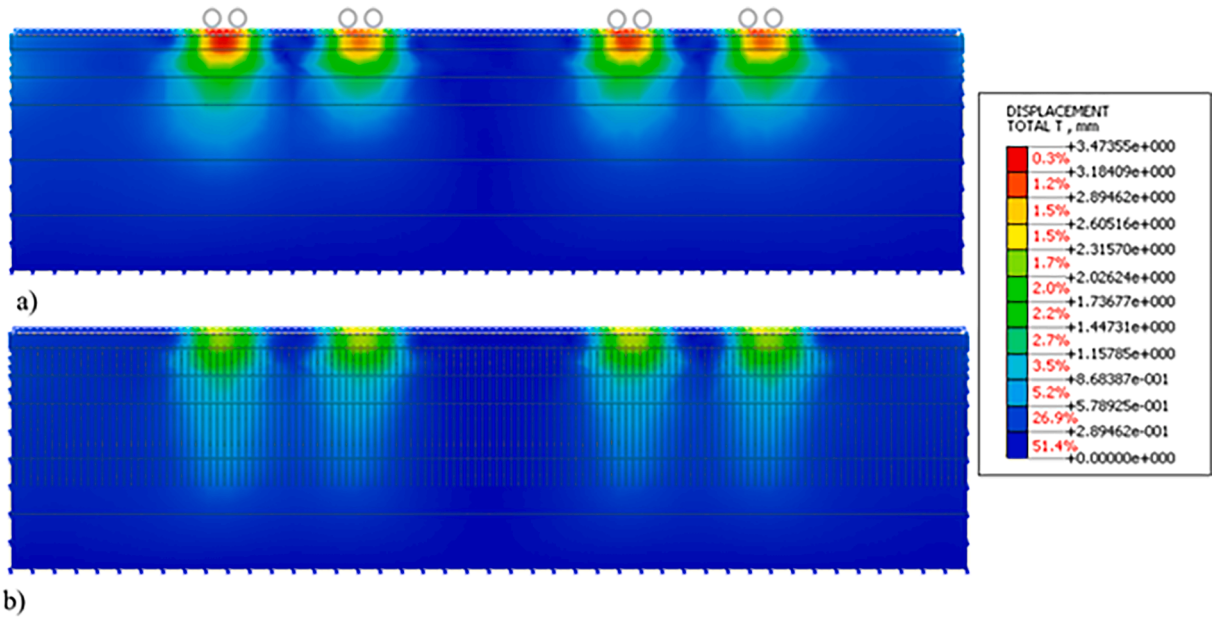

Fig 13. The contours of total displacement in the longitudinal section under train axles (grey circles), obtained by FE, for models of; a) pre-micro-piling and b) post-micro-piling scenarios.

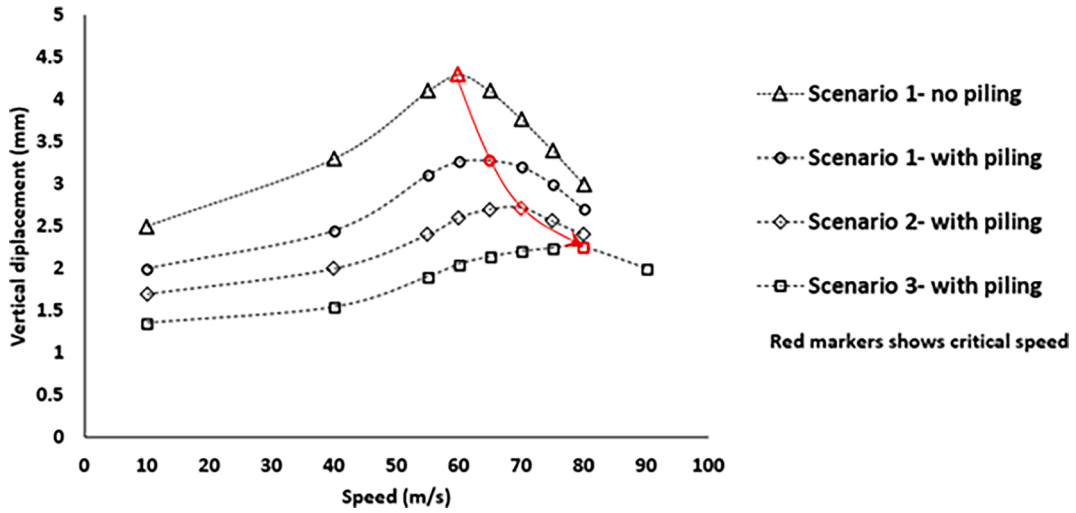

Fig 14. Evolution of track deflection versus train speed before and after stabilisation (micro-piling) to estimate the critical speed.

observed in the previous studies [32]. Fig. 15b (C) and 15b (D) show displacement response of ground at a train speed 60 m/s and 80 m/s, respectively, which are greater than the critical speed. For this case, the loading speeds are greater than the wave speeds and the source passes through wave fronts.

Therefore, it can be concluded that the efficacy of micro-piling is further improved by increasing ballast stiffness e.g., through renewal or other improvement, and by embedding pile toe within stiffer strata e.g., by increasing pile length.

3.9.2. Micro-pile arrangements

To optimise TBS design, four different arrangements of micro-piles were modelled. It should be noted that a car (with four axles) of the entire train was considered in the FE models to reduce the computation time. The ideal condition with clean ballast and relatively stiff soil-bed (stiff layer at Clay 3, Scenario 3) was considered for optimisation. Fig. 16a illustrates various pile arrangements in FE models, where A is a typical pile pair arrangement, B with additional piling in the centre of alignment, C is pile pair every other sleeper, and D is a triangular arrangement.

The vertical deflections of trackbed stabilised by the aforementioned arrangements were estimated using FE models (Fig. 16b). It can be seen that the maximum reduction (~51%) obtained where the additional piles installed in the middle of the track (B). Here, micro-piling in the triangular (D) and every other sleeper arrangement (C) cause respectively, 40% and 30% reduction in the vertical deformation compared to the trackbed before micro-piling. According to the results and considering the cost of manufacturing and installation of each pile, the triangular arrangement for pile installation can be considered as an optimised scenario.

This study did not attempt to simulate the effectiveness of the arching mechanism within dirty ballast, which would merit further studies using a different modelling approach. Furthermore, the research efforts in this paper were directed toward the bearing capacity of the trackbed; however, the installation and structural aspects of the proposed micro-pile foundation were neglected. Therefore, future research

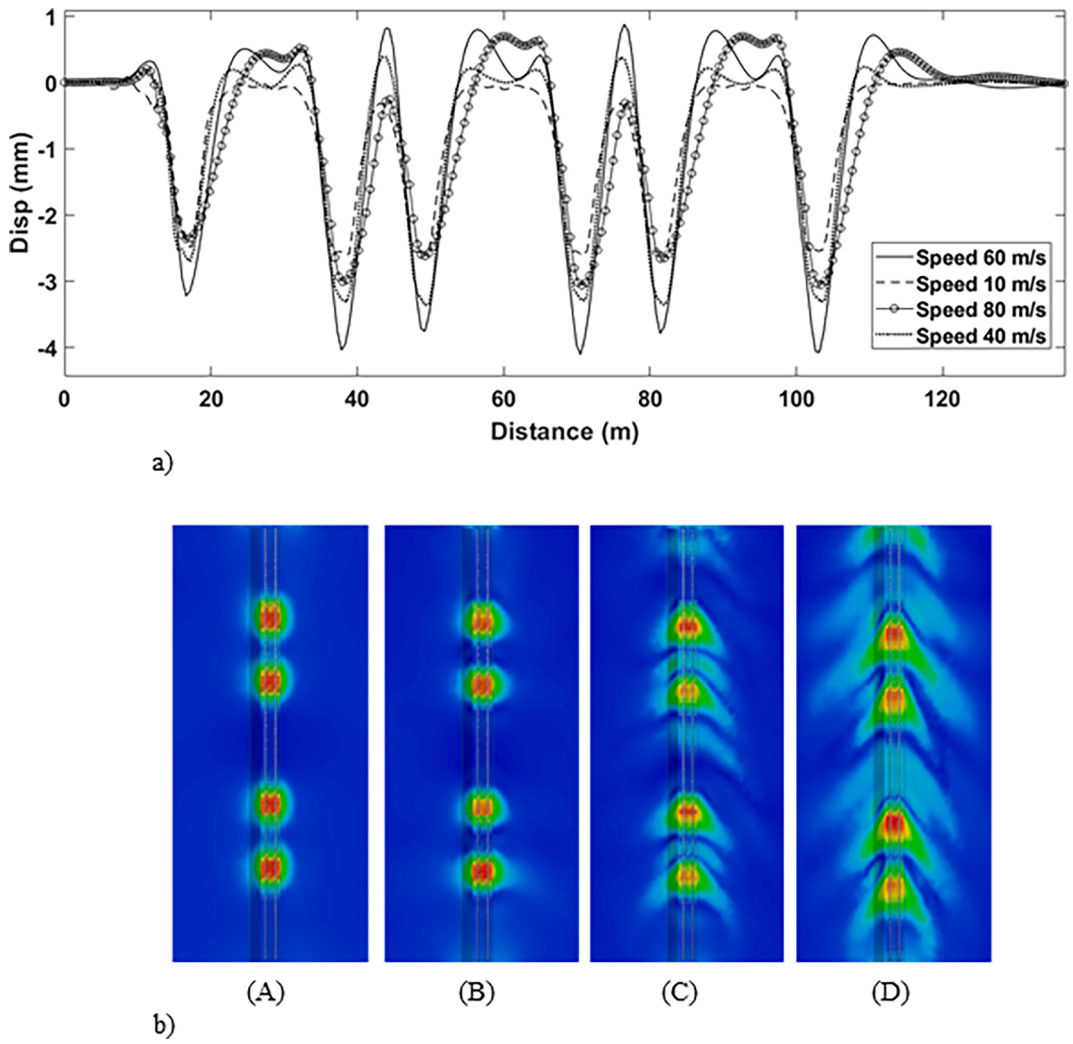

Fig 15. a) FE predicted for deflection responses at the track centre for various train speeds; and b) contour plots of plan view of total track deflection for the train speed of; (a) 10 m/s, (B) 40 m/s, (C) 60 m/s, and (D) 80 m/s.

is recommended to address potential structural and installation issues associated with the proposed TBS foundation.

4. Summary and conclusions

This study assessed the efficiency of micro-piling as a novel and minimal disruption trackbed stabilisation (TBS) technique for a pre-existing track in an area of low subgrade stiffness. A computer vision-based monitoring (VBM) system was used to measurement the track structure deflection both before and after micro-piling. The track modulus was calculated and used to quantify the improvement made by micro-piling. Finite element (FE) dynamic models were developed to scrutinise the dynamic response of the trackbed. The models were used to estimate micro-pile efficacy under different ballast and subgrade stiffnesses, pile arrangements, and for calculating the critical speed of the trackbed, consequently identifying an optimum design of micro-pling. This study draws the following conclusions:

- The developed VBM system is an efficient and accurate in-situ measurement system for obtaining displacement measurements of rails. These measurements can be directly related to the performance of the trackbed.
- The quality and stiffness of the trackbed are improved by approximately 20–30% after stabilisation with micro-piling. However, the effectiveness of the micro-piling system is dependent on the conditions of the ballast and sub-layers, where higher stiffness of these elements correspond with further improvement to track quality. It is important to consider the condition of the ballast and the length of the pile, as sometimes a hybrid stabilisation is needed to enhance trackbed performance to the needed level.
- According to the FE results, the pile arrangement can be altered to balance track quality improvements with cost and a triangular arrangement of piles was noted as the optimum solution in this study.

Although this study has described the efficacy of micro-piling for tracks with poor subgrade, other works, e.g., ballast improvement, may need to follow on and post TBS and careful monitoring is needed to identify this. Furthermore, the monitoring in this study was only for a limited period shortly after TBS and ideally long-term monitoring over several years would continue to identify the rate and degree of long-term degradation. Notwithstanding, where carefully designed and monitored to confirm performance, the micro-piling technique is an effective and lowly disruptive method to improve poor trackbeds, enhancing both the safety and efficiency of railway transportation.

CRediT authorship contribution statement

Koohyar Faizi: Writing – original draft, Validation, Software, Resources, Methodology, Formal analysis. **Paul Beetham:** Writing – review & editing, Supervision. **Rolands Kromanis:** Writing – review &

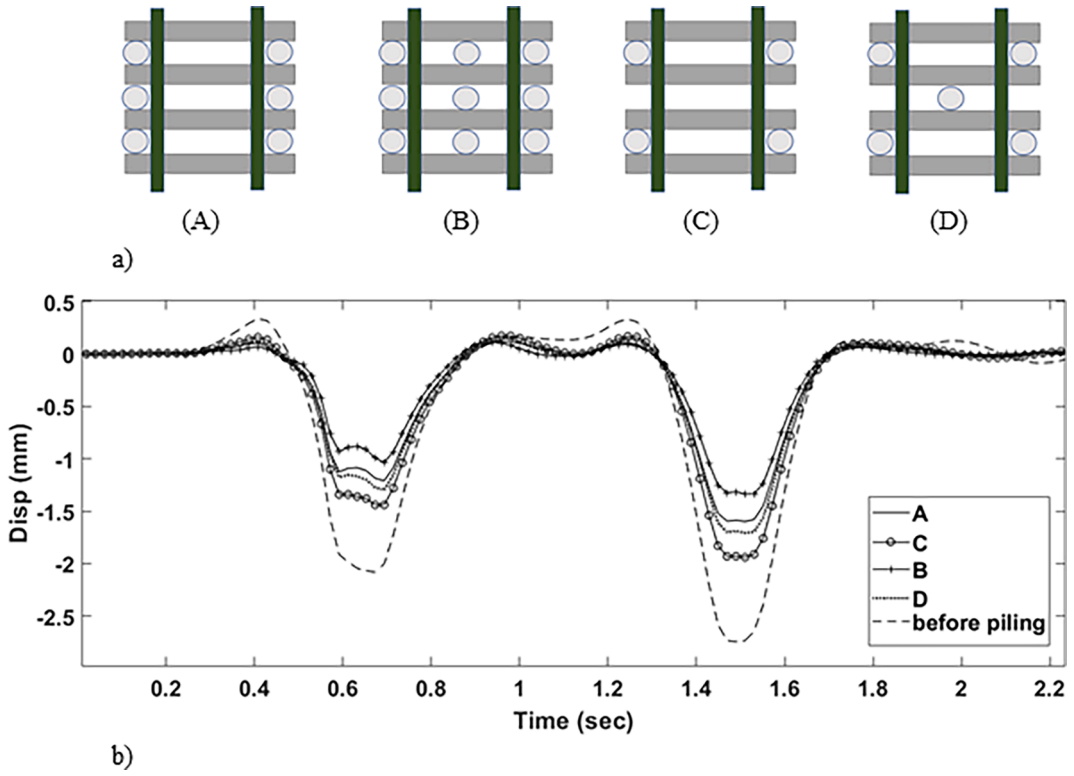

Fig 16. a) pile arrangement: (A) between each sleeper-on-sleeper ends; (B) between each sleeper on sleeper ends and in 4-foot; (C) every other sleeper on sleeper ends (D) triangular; b) vertical deflation vs time based on various pile arrangement.

editing, Supervision.

Declaration of Competing Interest

The authors declare the following financial interests/personal relationships which may be considered as potential competing interests: Koohyar Faizi reports financial support, administrative support, and equipment, drugs, or supplies were provided by Van Elle ltd.

Data availability

The authors do not have permission to share data.

Acknowledgements

This Knowledge Transfer Partnership (KTP) project is funded by UKRI through Innovate UK with the support of co-founders, including the Van Elle Ltd. The KTPs aim to help businesses improve their competitiveness and productivity through better use of the knowledge, technology and skills held within the UK knowledge base. The authors are grateful for the valuable support of John Allsop, the Engineering Director for Rail at Van Elle in conducting the field validation and monitoring experiments.

References

[1] Manual of GTS-NX, v1.2: new experience of geotechnical analysis system, MIDAS Company Limited, South Korea. (2013).
[2] S. Aingaran, L. le Pen, A. Zervos, W. Powrie, Modelling the effects of trafficking and tamping on scaled railway ballast in triaxial tests, Transportation Geotechnics 15 (2018) 84–90.
[3] ARAÚJO, N. M. F. 2011. High-speed trains on ballasted railway track: dynamic stress field analysis.
[4] D.M. Barbieri, M. Tangerås, E. Kassa, I. Hoff, Z. Liu, F. Wang, Railway ballast stabilising agents: Comparison of mechanical properties, Construction and Building Materials 252 (2020), 119041.
[5] D. Bowness, A. Lock, W. Powrie, J. Priest, D. Richards, Monitoring the dynamic displacements of railway track, Proceedings of the Institution of Mechanical Engineers, Part F: Journal of Rail and Rapid Transit 221 (2007) 13–22.
[6] J.M.W. Brownjohn, Y. Xu, D. Hester, Vision-based bridge deformation monitoring, Frontiers in Built Environment 3 (2017) 23.
[7] K. Faizi, M. Gallou, J. Allsop, M. Brough, RAIL TRACKBED STABILISATION USING MICRO-PILING, Permanent Way Institute Journal. (2023).
[8] Faizi, K., Kromanis, R., Beetham, P. & Allsop, J. The Resilience of Vision-Based Technology for Railway Track bed Monitoring. In: POMBO, J., ed. The Fifth International Conference on Railway Technology: Research, Development and Maintenance, Montpellier, France, Civil-Comp Ltd, Edinburgh, UK, 2022, p. 2022.
[9] V. Galavi, R. Brinkgreve, Finite element modelling of geotechnical structures subjected to moving loads, Numerical Methods in Geotechnical Engineering (2014) 235–240.
[10] S.H. Ju, S.H. Ni, Determining Rayleigh damping parameters of soils for finite element analysis, International journal for numerical and analytical methods in geomechanics 31 (2007) 1239–1255.
[11] E. Kausel, J. Estaire, I. Crespo-Chacón, Proof of critical speed of high-speed rail underlain by stratified media, Proceedings of the Royal Society A 476 (2020) 20200083.
[12] KAYES, I., NISSEN, D. & ADAMSON, J. Stabilisation of rail track formation and embankments. CORE 2000, Railway Technology for the 21st Century, Conference on Railway Engineering, Glenelg, South Australia, May 21-23, 2000, 2000.
[14] G. Kouroussis, O. Verlinden, C. Conti, Finite-dynamic model for infinite media: corrected solution of viscous boundary efficiency, Journal of Engineering Mechanics 137 (2011) 509–511.
[15] R. Kromanis, P. Kripakaran, A multiple camera position approach for accurate displacement measurement using computer vision, Journal of Civil Structural Health Monitoring 11 (2021) 661–678.
[16] J. Lysmer, R.L. Kuhlemeyer, Finite dynamic model for infinite media, Journal of the engineering mechanics division 95 (1969) 859–877.
[17] C. Miao, Y. Jia, J. Zhang, J. Zhao, DEM simulation of the pullout behavior of geogrid-stabilized ballast with the optimization of the coordination between aperture size and particle diameter, Construction and Building Materials 255 (2020), 119359.
[18] D. Milne, L. le Pen, G. Watson, D. Thompson, W. Powrie, M. Hayward, S. Morley, Monitoring and repair of isolated trackbed defects on a ballasted railway, Transportation Geotechnics 17 (2018) 61–68.
[19] D. Milne, L.L. Pen, D. Thompson, W. Powrie, Automated processing of railway track deflection signals obtained from velocity and acceleration measurements, Proceedings of the Institution of Mechanical Engineers, Part F: Journal of Rail and Rapid Transit 232 (2018) 2097–2110.
[20] C.A. Murray, W.A. Take, N.A. Hoult, Measurement of vertical and longitudinal rail displacements using digital image correlation, Canadian Geotechnical Journal 52 (2015) 141–155.

[21] MUSGRAVE, P., WEHBI, M., JACKSON, L., STEVENSON, A. & O'NEIL, L. 2017. A Guide to Track bed Micro Piling. Network Rail.
[22] P. Negi, R. Kromanis, A.G. Dorée, K.M. Wijnberg, Structural health monitoring of inland navigation structures and ports: a review on developments and challenges, Structural Health Monitoring 14759217231170742 (2023).
[23] N.T. Ngo, B. Indraratna, C. Rujikiatkamjorn, Stabilization of track substructure with geo-inclusions—experimental evidence and DEM simulation, International Journal of Rail Transportation 5 (2017) 63–86.
[24] Prakoso, p. b., Analysis and Evaluation of Railway Track Systems on Soft Soil: Trackbed Thickness Design and Dynamic Track-Soil Interaction, Technische Universität München, 2017.
[25] J. Priest, W. Powrie, Determination of dynamic track modulus from measurement of track velocity during train passage, Journal of geotechnical and geoenvironmental engineering 135 (2009) 1732–1740.
[26] J. Priest, W. Powrie, L. Yang, P. Grabe, C. Clayton, Measurements of transient ground movements below a ballasted railway line, Géotechnique 60 (2010) 667–677.
[27] PYE, N., O'BRIEN, A., ESSLER, R. & ADAMS, D. 2012. Deep dry soil mixing to stabilize a live railway embankment across Thrandeston Bog. *Grouting and Deep Mixing 2012*.
[28] Raymond, g. p., Analysis of track support and determination of track modulus, Transportation Research Record 1022 (1985) 80–90.
[29] M.A. Sayeed, M.A. Shahin, Three-dimensional numerical modelling of ballasted railway track foundations for high-speed trains with special reference to critical speed, Transportation Geotechnics 6 (2016) 55–65.
[30] E.T. Selig, D. Li, Track modulus: Its meaning and factors influencing it, Transportation Research Record 1470 (1994) 47–54.
[31] STARK, T. D., WILK, S. T., THOMPSON, H. B., SUSSMANN JR, T. R., BAKER, M. & HO, C. L. Evaluating fouled ballast using seismic surface waves. ASME/IEEE Joint Rail Conference, 2016. American Society of Mechanical Engineers, V001T01A002.
[32] Q. Sun, B. Indraratna, J. Grant, Numerical simulation of the dynamic response of ballasted track overlying a tire-reinforced capping layer. *Frontiers*, Built Environment 6 (2020).
[33] Takemiya, h., Simulation of track–ground vibrations due to a high-speed train: the case of X-2000 at Ledsgard, Journal of Sound and Vibration 261 (2003) 503–526.
[34] K.M. Tappenden, D.C. Sego, Predicting the axial capacity of screw piles installed in Canadian soils, The Canadian Geotechnical Society (CGS), OttawaGeo2007 Conference (2007) 1608–1615.
[35] B.J. van Dyk, J.R. Edwards, M.S. Dersch, Ruppert jr, c. j. & barkan, c. p., Evaluation of dynamic and impact wheel load factors and their application in design processes, Proceedings of the Institution of Mechanical Engineers, Part F: Journal of Rail and Rapid Transit 231 (2017) 33–43.
[36] WANG, H., MARKINE, V. & LIU, X. 2018. Experimental analysis of railway track settlement in transition zones. *Proceedings of the Institution of Mechanical Engineers, Part F: Journal of rail and rapid transit,* 232**,** 1774-1789.
[37] L.N. Wheeler, W.A. Take, N.A. Hoult, Performance assessment of peat rail subgrade before and after mass stabilization, Canadian Geotechnical Journal 54 (2017) 674–689.
[38] Y. Xu, J.M. Brownjohn, Review of machine-vision based methodologies for displacement measurement in civil structures, Journal of Civil Structural Health Monitoring 8 (2018) 91–110.